ACS APPLIED MATERIALS & INTERFACES

Research Article

www.acsami.org

Recovering Magnetic Fe_3O_4–ZnO Nanocomposites from Algal Biomass Based on Hydrophobicity Shift under UV Irradiation

Shijian Ge,[†] Michael Agbakpe,[†] Wen Zhang,*[,†] Liyuan Kuang,[†] Zhiyi Wu,[‡] and Xianqin Wang[‡]

[†]John A. Reif, Jr., Department of Civil and Environmental Engineering, New Jersey Institute of Technology, Newark, New Jersey 07102, United States

[‡]Department of Chemical Biological and Pharmaceutical Engineering, New Jersey Institute of Technology, Newark, New Jersey 07102, United States

Supporting Information

ABSTRACT: Magnetic separation, one of the promising bioseparation technologies, faces the challenges in recovery and reuse of magnetic agents during algal harvesting for biofuel extraction. This study synthesized a steric acid (SA)-coated Fe_3O_4–ZnO nanocomposite that could shift hydrophobicity under UV_{365} irradiation. Our results showed that with the transition of surface hydrophobicity under UV_{365} irradiation, magnetic nanocomposites detached from the concentrated algal biomass. The detachment was partially induced by the oxidation of SA coating layers due to the generation of radicals (e.g., $^{\bullet}OH$) by ZnO under UV_{365} illumination. Consequently, the nanocomposite surface shifted from hydrophobic to hydrophilic, which significantly reduced the adhesion between magnetic particles and algae as predicted by the extended Derjaguin and Landau, Verwey, and Overbeek (EDLVO) theory. Such unique hydrophobicity shift may also find many other potential applications that require recovery, recycle, and reuse of valuable nanomaterials to increase sustainability and economically viability.

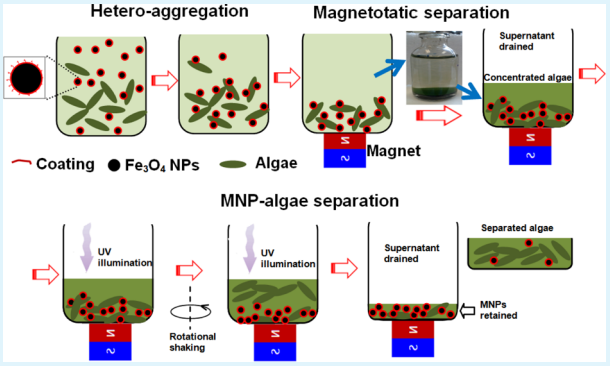

KEYWORDS: *magnetophoretic separation, magnetic nanoparticles, microalgae, algal harvesting, biofuel, hydrophobicity*

INTRODUCTION

Engineered magnetic nanomaterials or nanoparticles (NPs) are widely used in bioseparation, such as identification and separation of pathogenic cells, viruses, and proteins in water treatment and biomedical applications. More recently, magnetic separation of algal biomass for biofuel processing has gained much attention. Compared to traditional chemical coagulation and flocculation, magnephoretic separation using magnetic particles or nanoparticles (MNPs) seems more promising, because of low dose demand, high separation efficiency and potential to recover and reuse the magnetic agents.[1−6] Of the numerous critical challenges in magnetophoretic algal separation that must be overcome, recovery and reuse of MNPs are two major issues for securing the sustainability of this technology and reducing cost and potential contamination to algal biomass. For instance, the cost of MNPs and polymer binders could contribute approximately 33% to the total cost of magnetophoretic algal separation.[2] Nevertheless, there has been little research that investigated the separation and collection of magnetic NPs from the concentrated algal slurry.

Detachment of MNPs from algae may occur when MNPs or algal cells shift in either surface charge or surface wetting properties, leading to repulsion between them at the interface. Thus, the recovery of MNPs from algae in previous studies was achieved by heating or adding acid or base into the mixture to dissolve MNPs or detach MNPs from algae.[7−9] For example, MNPs were dissolved by HCl and algae (*Chlorella ellipsoidea*) were separated by microfiltration with filtrate reused for Fe_3O_4 synthesis.[9] Prochazkova et al. reported that detachment of iron oxide NPs from algae (*Chara vulgaris*) in 10 mM KCl at pH 12 with detachment efficiencies from 10 to 90%.[8] Also, the algae-iron oxide NPs aggregates could be dissolved with 10 vol % H_2SO_4 by heating (40 °C) with/without ultrasonication to purify the harvested algal cells.[10] Clearly, as hazardous chemicals, the use of acids or base to adjust solution pH may not be environmentally sustainable or economically feasible. Likewise, heating is not practical for large-scale algal production.[9] By contrast, our previous studies have attempted to mechanically separate MNPs through a chemical-free method with ultrasonication.[6,11] Briefly, the MNPs-algae slurry was sonicated in the ice bath. The detached MNPs were further separated from algal biomass by a magnet. The slurry containing the majority of algae and a small fraction of MNPs was decanted after magnetic separation. Because of the strong binding, the detachment and separation efficiencies of MNPs from algae through mechanical agitation are still limited.

Received: April 21, 2015
Accepted: May 12, 2015
Published: May 12, 2015

DOI: 10.1021/acsami.5b03472
ACS Appl. Mater. Interfaces 2015, 7, 11677−11682

As mentioned above, another potential pathway to detach MNPs from algae is to tune surface wetting properties (hydrophobicity or hydrophilicity) of MNPs or algae. Typically, we engineer MNPs (not algae) via surface coating or functionalization to achieve desirable surface characteristics. Common surface coatings on MNPs include positively or negatively charged polyelectrolytes[12,13] and hydrophobic or hydrophilic polymers.[2,14,15] Recently, surface hydrophobicity of some nanomaterials (e.g., ZnO) was found to shift under UV illumination or temperature changes.[16−18] For example, ZnO nanorods coated with fluoroalkyl and alkyl silanes were demonstrated to reversibly transit wetting properties under UV irradiation (248−365 nm).[19] Superparamagnetic iron oxide microspheres with amine coating and dendrimer and silver mesodendritic structure coated zinc substrate were both reported to have reversible switch of surface wettability.[20,21] To the best of our knowledge, no studies have applied this feature of (reversible) transition of surface hydrophobicity to separate magnetic agents from algal cells, which may lead to intriguing algal harvesting and MNP recovery processes.

In this study, MNPs were built by depositing the superparamagnetic magnetic (Fe_3O_4) NPs onto ZnO, which was further decorated with steric acid (SA, $CH_3(CH_2)_{16}COOH$). The expected benefits are that the coatings of ZnO and SA may prevent aggregation and oxidation of the magnetic NPs. Further, ZnO with bandgap of around 3.37 eV could catalyze the generation of radicals (e.g., $OH^{\bullet}$) under UV illuminaton.[22−26] The radicals should oxidize the SA molecules on the surface of MNPs and alter hydrophobicity as well as the interactions between MNPs and algae. The shift in surface hydrophobicity under UV illumination may promote the recovery of MNPs from algal slurry. To prove this above hypothesis, we carried out a series of experiment as detailed in the Supporting Information (SI). The aim of this research is to present a prototype model for simultaneous algal harvesting and recovery of magnetic agents.

MATERIALS AND METHODS

Cultivation and Preparation of Algal Suspension. Our algal cells (*Scenedesmus dimorphus*) was cultivated in the modified Bold's basal medium (MBBM) with details reported in our previous works.[1,6,11] The initial inoculated algal concentration was approximately 0.2 g·L^{-1} as characterized by the dry cell weight (DCW). The final steady-state algal concentration after 14-day incubation was around 1.8 g·L^{-1}.

Preparation of magnetic magnetite or Fe_3O_4 NPs synthesis. We followed the same synthesis protocol that was reported previously.[4] The obtained magnetite powder at 20 g-NPs L^{-1} was dispersed in 5 M steric acid solution dissolved in ethanol, followed by sonication for 30 min for good dispersion. The steric-acid molecules (Fisher Scientific, USA) were allowed to chemisorb on the NPs surface for 24 h. Then, the precipitate was collected using magnet and washed three times with deionized (DI) water and ethanol to remove excessive lactic groups adsorbed on MNPs. Then, the resultant material was oven-dried at 60 °C for 24 h.

Surface Modification of Fe_3O_4−ZnO Nanocomposites with Steric Acid. In this step, 0.7 g of SA-modified magnetite NPs were ultrasonically dispersed in DI for 15 min. Then, 0.5 g of ZnO NPs (approximately 50 nm in diameter) purchased by Sigma-Aldrich was added and kept under ultrasonic irradiation for 15 min. After this step, under continuous magnetic stirring for 2 h, SA-modified magnetite NPs adsorbed onto ZnO. Then, the samples were oven-dried at 50 °C for 24 h to be prepared for characterization.

Algal harvesting and detaching experiments. After 14-day cultivation, the algal suspension in the culture medium was directly used in the magnetophoretic separation experiments. The SA-coated Fe_3O_4−ZnO nanocomposite was directly applied at a loading rate of 0.3 g-MNPs·g-algae^{-1} to the algal suspension in a 25-mL glass specimen bottle with the initial algal concentration of 0.8 g L^{-1}. After rigorous mixing for 2 min,[9] a NdFeB permanent magnet (K&J Magnetics, Inc.) was placed under the bottle for 3 min to separate the MNPs-algae aggregates. The maximum surface magnetic field was 0.175 T as measured by a magnetometer (PS-2112, PASCO). The optical density of the algal suspension at 680 nm (OD_{680}) was measured to quantify the concentrations of algae. To recover the nanocomposite from algal biomass, first we discarded half (10 mL) of the suspension (the clear supernatant). The remaining concentrated algae-NPs aggregates on the bottom were evenly transferred into four 96 mm Petri dishes to act as different test groups (i.e., the control, only mixing, UV and mixing, and only UV). Then, two Petri dishes were exposed to the 365 nm UV irradiation of 3.2 mW cm^{-2}, while the other two were placed in room light without UV irradiation. To evaluate the migration of algae from the aggregated clusters into the bulk suspension, the OD_{680} of supernatant was measured. The mass fractions of the resuspended algae cells out of the total algal biomass at different sampling times were determined.

UV-stimulated Conversion of Wettability. SA−Fe_3O_4−ZnO nanocomposites were placed under a 6-W mercury lamp, which emits UV light in the wavelength 356 nm. Fe_3O_4−ZnO nanocomposites was directly illuminated at the light intensity of 2.6 mW cm^{-2} in air at room temperature. Relative humidity was kept in all experiments at 40%. The water contact angle (CA) of the samples were measured as a function of the UV illumination time.

Characterization of SA-Coated Fe_3O_4−ZnO Nanocomposites and Algae. To measure the algal concentrations in the supernatant, liquid samples were taken for the optical absorbance measurement at 680 nm by a Thermo Scientific Evolution 201PC UV−vis spectrophotometer. The NPs concentration were represented by the total iron (Fe) concentration determined by an Agilent 7500i Benchtop Inductively Coupled Plasma-Mass Spectrometer System (ICP-MS). The morphology and sizes of the MNPs and algae cells were determined by a JEOL JSM-7100FA scanning electron microscope (SEM). Hydrodynamic size distribution (PSD) and zeta potential were measured by dynamic light scattering (DLS) on a Zetasizer nano ZS instrument (Malvern Instruments, UK). X-ray Diffraction (XRD) was recorded for the crystallography using a Philips PW3040 X-ray Diffractometer. Surface compositions were assessed by Fourier Transform Infrared (FTIR) and Raman Spectrometers. FTIR was performed on a Nicolet ThermoElectron FTIR spectrometer combined with a MIRacle attenuated total reflectance (ATR) platform assembly and a Ge plate, while Raman was carried out with a Thermo Scientific DXR Raman microscope using an argon ion laser excitation (λ = 514.5 nm) at powers of 2−10 mW.

Statistical Analysis. All algal harvesting and magnetic nanocomposite recovery experiments were carried out at room temperature of 25 ± 3 °C with triplicate sampling and testing. The presented results are mean values ± standard deviation from three independent experiments.

RESULTS AND DISCUSSION

Characterization. Briefly, surface element compositions and morphology of SA-coated Fe_3O_4−ZnO nanocomposite itself and the nanocomposite adsorbed on algae are shown in Figure 1. Figure 1a indicates the nanocomposite had elements, such as iron, zinc, as well as carbon and oxygen, which likely originated from the SA molecules. The inset of Figure 1b shows the SEM image of aggregated clusters of algae and the nanocomposite clusters. The EDS spectrum of this mixture in Figure 1b indicates the presence of some new elements such as Mg, Na, P, and S, which probably resulted from algal surface function groups (e.g., sulfhydryl groups) or the residuals of the algal medium. The XRD patterns of Fe_3O_4, ZnO, and SA-coated Fe_3O_4−ZnO nanocomposite are shown in Figure 2,

DOI: 10.1021/acsami.5b03472
ACS Appl. Mater. Interfaces 2015, 7, 11677−11682

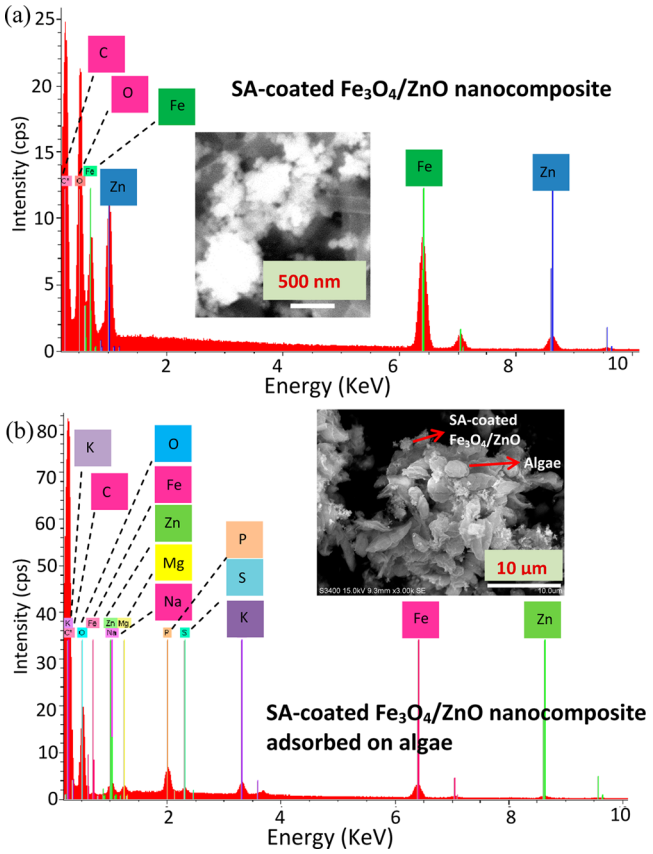

Figure 1. EDS spectra for (a) SA-coated Fe_3O_4–ZnO nanocomposite adsorbed on algae and (b) the magnetic nanocomposite only. Insets of panels a and b are SEM images of magnetic nanocomposite particles and the mixture with algae.

which well matched the standard patterns of ZnO (JCPDF 00-036-1451) and Fe_3O_4 (JCPDF 01-075-0033).

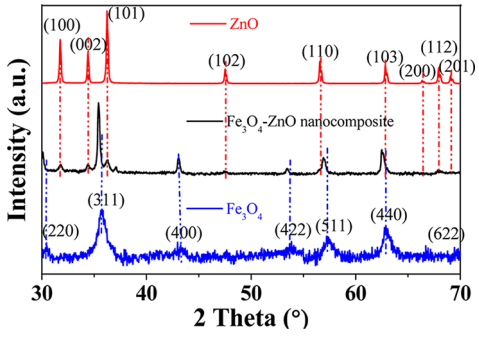

Figure 2. XRD patterns for ZnO, Fe_3O_4, and Fe_3O_4–ZnO nanocomposite.

The FTIR and Raman spectra shown in Figure 3 are used to confirm the presence of SA and ZnO on Fe_3O_4 NPs. Bare or naked Fe_3O_4 NPs had a strong peak at around 600–700 cm^{-1}, which is attributed to the Fe–O stretching mode of the tetrahedral and octahedral sites.[27] The peaks at around 1500 cm^{-1} could be attributed to the stretching or bending vibrations of O–H. With the SA coating, the changes of FTIR spectra was not evident, although the C═O stretching vibration band at 1702 cm^{-1} is expected due to the presence of the carboxylic acid groups in stearic acid. After decoration of ZnO, a sharp

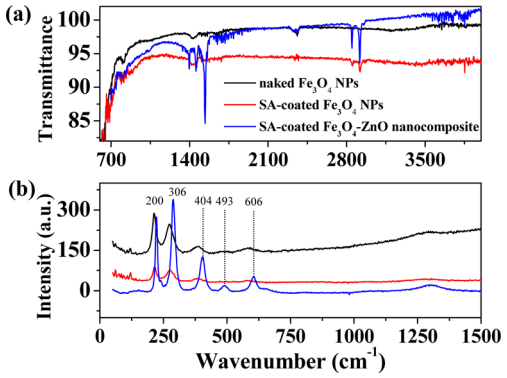

Figure 3. (a) FTIR specta and (b) Raman spectra of naked Fe_3O_4, SA-coated Fe_3O_4 NPs, and SA-coated Fe_3O_4–ZnO nanocomposite.

peak appeared at around 1420, 1470, and 1540 cm^{-1}, which are due to stretching vibration of O–H, bending modes of C–H, and stretching modes of COO^-.[28] The intensity of the peaks at 2838 and 2919 cm^{-1} also increased significantly. The Raman spectra for naked Fe_3O_4 NPs and SA-coated Fe_3O_4 NPs are almost identical, with apparent peaks at around 200 and 306 cm^{-1}, which are assigned to the typical T2g modes of magnetite.[29] In the presence of ZnO, the above two peaks remained but had minor shifts. New peaks at around 404, 493, and 606 cm^{-1} appeared, which is probably due to the E_2 and $A_{1(LO)}$ mode of ZnO crystallite.[30]

Detachment of SA-Coated Fe_3O_4–ZnO Nanocomposite from Concentrated Algae under UV Irradiation. The detachment of SA-coated Fe_3O_4–ZnO nanocomposite from concentrated algal biomass is demonstrated in Figure 4, which compares the mass fractions of algae resuspended into the supernatant suspension over time under the influences of UV_{365} irradiation, magnetic field and mechanical stirring or mixing that was used to well suspend magnetic nanocomposite particles to increase their UV exposure. Clearly, algae gradually migrated into the bulk suspension as indicated by the increase of optical density at 680 nm (OD_{680}) and the mass fraction in Figure 4a under mixing (no UV) and UV irradiation and mixing. However, with only UV irradiation or no UV and no mixing, algae did not detach but tightly attracted to the bottom of the container by the magnetic force as illustrated in Figure 4b. The total depth of the concentrated algal suspension in the Petri dish was maintained at a shallow depth (about 2 cm) as shown in Figure 4b to permit the effective penetration and exposure of UV irradiation on magnetic nanocomposite. UV_{365} irradiation undoubtedly played a promoting role in the uncoupling of algae and magnetic nanocomposites, which is further analyzed in the following.

Surface Hydrophobicity Changes of SA-Coated Fe_3O_4–ZnO Nanocomposite under UV Irradiation. The effect of UV irradiation on the algal detachment from the aggregate clusters of algae and SA-coated Fe_3O_4–ZnO nanocomposite was plausibly attributed to the UV-induced surface hydrophobicity changes.[31] Figure 5a shows the water CA changes of SA-coated Fe_3O_4 NPs and SA-coated Fe_3O_4–ZnO nanocomposite as a function of UV_{365} illumination time. Apparently, the CA of SA-coated Fe_3O_4 NPs remained quite stable, indicating that there was no or negligible oxidation of SA. Conversely, the CA of SA-coated Fe_3O_4–ZnO nanocomposite gradually decreased from 125.6 ± 10.0 at 0 min to 70.2 ± 3.8 at 240 min, because the hydrophobic surface coating of SA on Fe_3O_4–ZnO nanocomposite was oxidized (e.g.,

DOI: 10.1021/acsami.5b03472
ACS Appl. Mater. Interfaces 2015, 7, 11677–11682

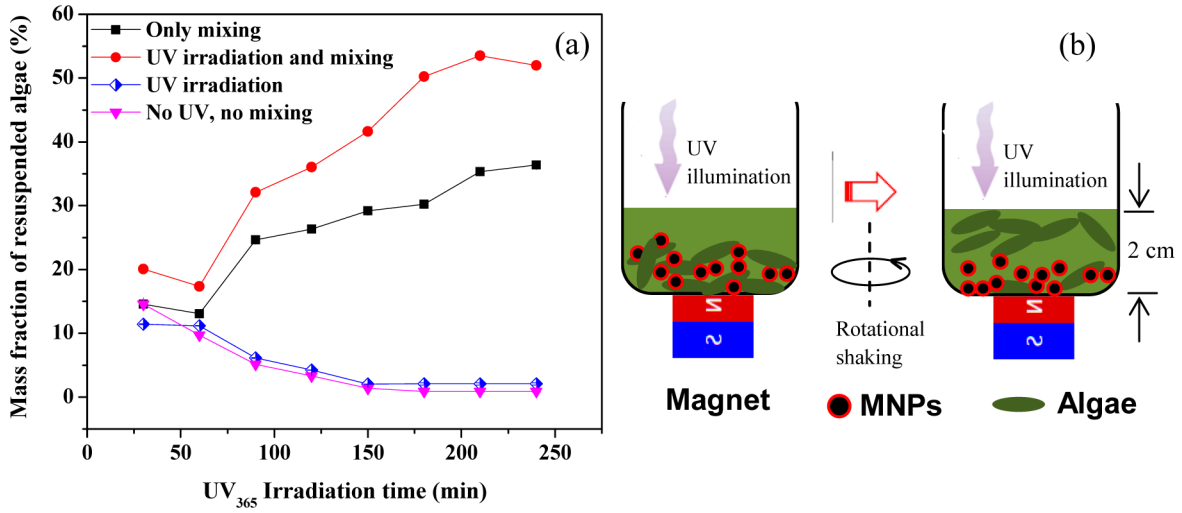

Figure 4. (a) Percentage of resuspended algae cells with different treatment methods. (b) Illustration of separation of algae or MNPs from aggregated clusters. Some error bars are too small to be visible.

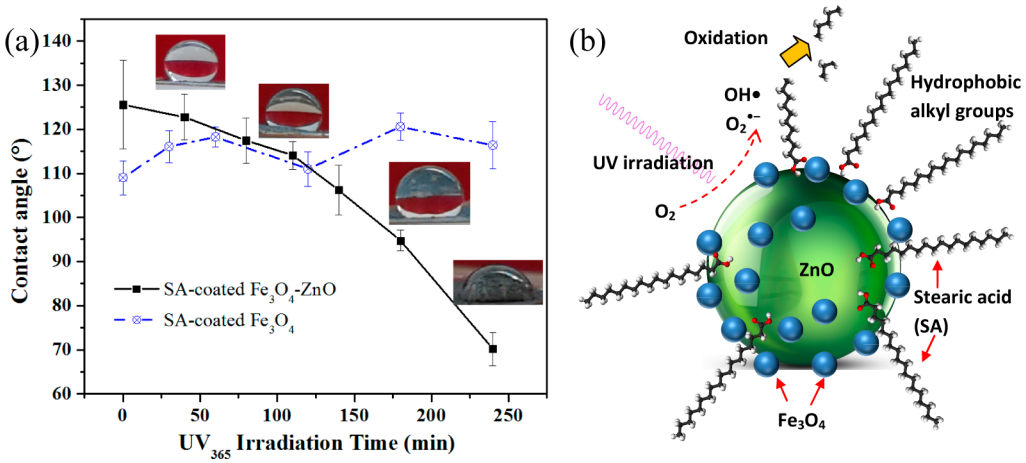

Figure 5. (a) Changes of water contact angles of SA-coated Fe_3O_4 and SA-coated Fe_3O_4–ZnO nanocomposites as a function of UV_{365} irradiation time. (b) Schematic of SA-coated Fe_3O_4–ZnO nanocomposite and oxidation of SA by ROS (e.g., $OH^{\bullet}$ and $O_2^{\bullet-}$) formed on ZnO.

hydrophobic alkyl to into hydrophilic groups such as carboxylate under the UV illumination).[31] Although some previous studies such as Ye et al.[32] and Cox et al.[33] reported that the organic coating (e.g., alkylsiloxane) could be slowly decomposed by direct UV exposure and radicals, our study demonstrated that the destructing effect of UV irradiation on the SA coating was not evident as revealed by results with the SA-coated Fe_3O_4 NPs. The photodecomposition of SA was likely due to the generation of reactive oxygen species (ROS) by the nanocomposite, especially by the ZnO core.[31] As shown in Figure 5b, ZnO, as a common semiconductor, may act as an effective catalyst on the surface of Fe_3O_4 and efficiently produce ROS under UV irradiation, which has been reported in our previous work.[25,34,35] As a strong and nonselective oxidant, $^{\bullet}OH$ among all the produced ROS, may particularly play the important role in the oxidization of the long chain SA into small fragments, which led to the shift from hydrophobicity to hydrophilicity on the surface of magnetic nanocomposite. In turn, the surface interaction energy between algae and magnetic nanocomposite would inevitably be altered (Figure 6), which could significantly affect the surface attachment or detachment of nanocomposite onto algae. Figure 6 compares the changes in interaction energies computed by the EDLVO theory with

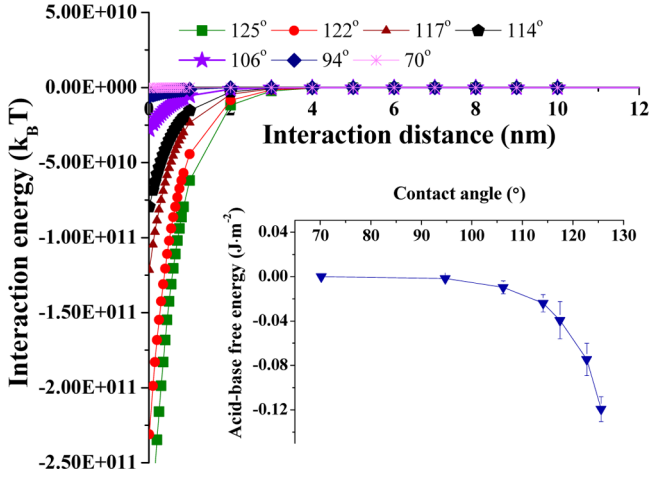

Figure 6. Total interaction energy as a function of the separation distance between algae and magnetic nanocomposite of different CAs. Inset shows the changes of the acid–base free energy with CA.

relevant equations shown in Supporting Information. Smaller contact angles (CA) resulted in more positive interaction

DOI: 10.1021/acsami.5b03472
ACS Appl. Mater. Interfaces 2015, 7, 11677–11682

energies, which means adhesion between algae and magnetic nanocomposite was reduced, thereby allowing algae to be released from the aggregated clusters on the bottom (see Figure 4b). The changes of surface interaction energy was primarily caused by the changes in the acid−base energy as shown in the inset of Figure 3, which is related to the surface hydrophobicity or CA according to eqs S3 and S4 in Supporting Information.

CONCLUSION

This work provides new insight that magnetic bioseparation techniques may become more sustainable with recovering and reusing magnetic agents, which are physically difficult to achieve at the present. A significant advantage of this recovery method over other reported approaches (e.g., acid/base addition to release or dissolve magnetic particles) is that this method avoids the use of hazardous chemicals and separates magnetic agents from algae "at the flick of a switch", simply with noninvasive UV irradiation. Importantly, this method better conserves the structures of magnetic NPs for reuse. Of course, there is still much work to improve, as magnetic particles may have to be coated by SA again, which has been oxidized to some extent. The future work may embrace two directions: (1) explore other organic polymer coating that can stabilize magnetic NPs and switch hydrophobicity reversibly under UV or other stimuli (e.g., electrical potential, heat, pH or selected solvents, and mechanical forces);[36] and (2) investigate the coating-free magnetic NPs that could demonstrate reversible hydrophobicity shift under UV. For instance, many nanomaterials, such as ZnO,[16] carbon nanotube,[37] and graphene,[38] have been shown to exhibit reversible magnetic NPs in air phase. However, in liquid phase, it is unknown if the switchable wettability of these materials could be retained, which is worth studying. Unraveling the mechanisms of surface interactions between algal cells and magnetic NPs is not only critical for improving algal harvesting processes using magnetophoresis, but also fundamentally important for physically enabling the recovery and reuse of magnetic NPs. The scientific insights and knowledge obtained in this study may not only promote the development of novel viable algal or biological separation processes but also other transformative applications in multifunctionalities including self-cleaning, antifouling surfaces, and stain resistant textiles. Particularly for membrane fabrication, functionalizing nanomaterials with switchable hydrophobicity properties on membrane surfaces may help reduce or resist fouling processes in wastewater/water treatment.

ASSOCIATED CONTENT

Supporting Information

EDLVO equations and Tables S1−S3. The Supporting Information is available free of charge on the ACS Publications website at DOI: 10.1021/acsami.5b03472.

AUTHOR INFORMATION

Corresponding Author

*E-mail: wzhang81@njit.edu. Phone: 1-973-596-5520. Fax: 1-973-596-5790.

Notes

The authors declare no competing financial interest.

ACKNOWLEDGMENTS

This study was supported by the Research Startup Fund at NJIT and National Science Foundation Grant CBET-1235166.

REFERENCES

(1) Ge, S.; Agbakpe, M.; Wu, Z.; Kuang, L.; Zhang, W.; Wang, X. Influences of Surface Coating, UV Irradiation and Magnetic Field on the Algae Removal Using Magnetite Nanoparticles. *Environ. Sci. Technol.* **2014**, *49*, 1190−1196.

(2) Toh, P. Y.; Yeap, S. P.; Kong, L. P.; Ng, B. W.; Chan, D. J. C.; Ahmad, A. L.; Lim, J. K. Magnetophoretic Removal of Microalgae from Fishpond Water: Feasibility of High Gradient and Low Fradient Magnetic separation. *Chem. Eng. J.* **2012**, *211*, 22−30.

(3) Lee, Y.-C.; Lee, K.; Hwang, Y.; Andersen, H. R.; Kim, B.; Lee, S. Y.; Choi, M.-H.; Park, J.-Y.; Han, Y.-K.; Oh, Y.-K. Aminoclay-templated Nanoscale Zero-Valent Iron (nZVI) Synthesis for Efficient Harvesting of Oleaginous Microalga, *Chlorella sp. KR-1*. *RSC Adv.* **2014**, *4*, 4122−4127.

(4) Hu, Y.-R.; Wang, F.; Wang, S.-K.; Liu, C.-Z.; Guo, C. Efficient Harvesting of Marine Microalgae *Nannochloropsis maritima* Using Magnetic Nanoparticles. *Bioresour. Technol.* **2013**, *138*, 387−390.

(5) Cerff, M.; Morweiser, M.; Dillschneider, R.; Michel, A.; Menzel, K.; Posten, C. Harvesting fresh water and marine algae by magnetic separation: screening of separation parameters and high gradient magnetic filtration. *Bioresour. Technol.* **2012**, *118*, 289−295.

(6) Ge, S.; Agbakpe, M.; Zhang, W.; Kuang, L. Heteroaggregation between PEI-coated Magnetic Nanoparticles and Algae: Effect of Particle Size on Algal Harvesting Efficiency. *ACS Appl. Mater. Interfaces* **2015**, *7*, 6102−6108.

(7) Seo, J. Y.; Lee, K.; Lee, S. Y.; Jeon, S. G.; Na, J.-G.; Oh, Y.-K.; Park, S. B. Effect of Barium Ferrite Particle Size on Detachment Efficiency in Magnetophoretic Harvesting of Oleaginous *Chlorella* sp. *Bioresour. Technol.* **2014**, *152*, 562−566.

(8) Prochazkova, G.; Podolova, N.; Safarik, I.; Zachleder, V.; Branyik, T. Physicochemical Approach to Freshwater Microalgae Harvesting with Magnetic Particles. *Colloids Surf., B* **2013**, *112*, 213−218.

(9) Xu, L.; Guo, C.; Wang, F.; Zheng, S.; Liu, C.-Z. A Simple and Rapid Harvesting Method for Microalgae by in Situ Magnetic Separation. *Bioresour. Technol.* **2011**, *102*, 10047−10051.

(10) Prochazkova, G.; Safarik, I.; Branyik, T. Harvesting Microalgae with Microwave Synthesized Magnetic Microparticles. *Bioresour. Technol.* **2013**, *130*, 472−477.

(11) Agbakpe, M.; Ge, S.; Zhang, W.; Zhang, X.; Kobylarz, P. Algae Harvesting for Biofuel Production: Influences of UV Irradiation and Polyethylenimine (PEI) Coating on Bacterial Biocoagulation. *Bioresour. Technol.* **2014**, *166*, 266−272.

(12) Wilhelm, C.; Billotey, C.; Roger, J.; Pons, J.; Bacri, J.-C.; Gazeau, F. Intracellular Uptake of Anionic Superparamagnetic Nanoparticles as a Function of Their Surface Coating. *Biomaterials* **2003**, *24*, 1001−1011.

(13) Moffat, B. A.; Reddy, G. R.; McConville, P.; Hall, D. E.; Chenevert, T. L.; Kopelman, R. R.; Philbert, M.; Weissleder, R.; Rehemtulla, A.; Ross, B. D. A Novel Polyacrylamide Magnetic Nanoparticle Contrast Agent for Molecular Imaging Using MRI. *Mol. Imaging* **2003**, *2*, 324−332.

(14) Tang, S. C.; Lo, I. M. Magnetic Nanoparticles: Essential Factors For Sustainable Environmental Applications. *Water Res.* **2013**, *47*, 2613−2632.

(15) Mikhaylova, M.; Kim, D. K.; Bobrysheva, N.; Osmolowsky, M.; Semenov, V.; Tsakalakos, T.; Muhammed, M. Superparamagnetism of Magnetite Nanoparticles: Dependence on Surface Modification. *Langmuir* **2004**, *20*, 2472−2477.

(16) Feng, X.; Feng, L.; Jin, M.; Zhai, J.; Jiang, L.; Zhu, D. Reversible Super-Hydrophobicity to Super-Hydrophilicity Transition of Aligned ZnO Nanorod Films. *J. Am. Chem. Soc.* **2004**, *126*, 62−63.

(17) Zhang, X.; Kono, H.; Liu, Z.; Nishimoto, S.; Tryk, D. A.; Murakami, T.; Sakai, H.; Abe, M.; Fujishima, A. A Transparent and

DOI: 10.1021/acsami.5b03472
ACS Appl. Mater. Interfaces 2015, 7, 11677−11682

Photo-Patternable Superhydrophobic Film. *Chem. Commun.* **2007**, 4949−4951.
(18) Oliveira, S. M.; Alves, N. M.; Mano, J. F. Cell Interactions with Superhydrophilic and Superhydrophobic Surfaces. *J. Adhes. Sci. Technol.* **2014**, *28*, 843−863.
(19) Liu, Y.; Lin, Z.; Lin, W.; Moon, K. S.; Wong, C. P. Reversible Superhydrophobic−Superhydrophilic Transition of ZnO Nanorod/Epoxy Composite Films. *ACS Appl. Mater. Interfaces* **2012**, *4*, 3959−3964.
(20) Leung, K. C.-F.; Xuan, S.; Lo, C.-M. Reversible Switching between Hydrophilic and Hydrophobic Superparamagnetic Iron Oxide Microspheres via One-Step Supramolecular Dynamic Dendronization: Exploration of Dynamic Wettability. *ACS Appl. Mater. Interfaces* **2009**, *1*, 2005−2012.
(21) Gao, Y.; Xia, B.; Liu, J.; Ding, L.; Li, B.; Zhou, Y. Reversible Tuning of the Wettability on a Silver Mesodendritic Surface by the Formation and Disruption of Lipid-like Bilayers. *Appl. Surf. Sci.* **2015**, *329*, 150−157.
(22) Ahadpour Shal, A.; Jafari, A. Study of Structural and Magnetic Properties of Superparamagnetic Fe_3O_4−ZnO Core−Shell Nanoparticles. *J. Supercond. Novel Magn.* **2014**, *27*, 1531−1538.
(23) Wu, W.; He, Q.; Jiang, C. Magnetic Iron Oxide Nanoparticles: Synthesis and Surface Functionalization Strategies. *Nanoscale Res. Lett.* **2008**, *3*, 397−415.
(24) Li, Y.; Niu, J.; Zhang, W.; Zhang, L.; Shang, E. Influence of Aqueous Media on the ROS-Mediated Toxicity of ZnO Nanoparticles toward Green Fluorescent Protein-Expressing *Escherichia coli* under UV-365 Irradiation. *Langmuir* **2014**, *30*, 2852−2862.
(25) Li, Y.; Zhang, W.; Niu, J.; Chen, Y. Mechanism of Photogenerated Reactive Oxygen Species and Correlation with the Antibacterial Properties of Engineered Metal−Oxide Nanoparticles. *ACS Nano* **2012**, *6*, 5164−5173.
(26) Zhang, W.; Li, Y.; Niu, J.; Chen, Y. Photogeneration of Reactive Oxygen Species on Uncoated Silver, Gold, Nickel, and Silicon Nanoparticles and Their Antibacterial Effects. *Langmuir* **2013**, *29*, 4647−4651.
(27) Jafari, A.; Boustani, K.; Shayesteh, S. F. Effect of Carbon Shell on The Structural and Magnetic Properties of Fe_3O_4 Superparamagnetic Nanoparticles. *J. Supercond. Novel Magn.* **2014**, *27*, 187−194.
(28) Singh, S.; Barick, K. C.; Bahadur, D. Fe_3O_4 Embedded ZnO Nanocomposites For The Removal of Toxic Metal Ions, Organic Dyes and Bacterial Pathogens. *J. Mater. Chem. A* **2013**, *1*, 3325−3333.
(29) Shebanova, O. N.; Lazor, P. Raman Spectroscopic Study of Magnetite ($FeFe_2O_4$): A New Assignment For The Vibrational Spectrum. *J. Solid State Chem.* **2003**, *174*, 424−430.
(30) Huang, Y.; Liu, M.; Li, Z.; Zeng, Y.; Liu, S. Raman Spectroscopy Study of ZnO-based Ceramic Films Fabricated by Novel Sol−Gel Process. *Mater. Sci. Eng., B* **2003**, *97*, 111−116.
(31) Kwak, G.; Seol, M.; Tak, Y.; Yong, K. Superhydrophobic ZnO Nanowire Surface: Chemical Modification and Effects of UV Irradiation. *J. Phys. Chem. C* **2009**, *113*, 12085−12089.
(32) Ye, T.; Wynn, D.; Dudek, R.; Borguet, E. Photoreactivity of Alkylsiloxane Self-assembled Monolayers On Silicon Oxide Surfaces. *Langmuir* **2001**, *17*, 4497−4500.
(33) Cox, R. A.; Patrick, K. F.; Chant, S. A. Mechanism of Atmospheric Photooxidation of Organic Compounds. Reactions of Alkoxy Radicals in Oxidation of *n*-butane And Simple Ketones. *Environ. Sci. Technol.* **1981**, *15*, 587−592.
(34) Zhang, W.; Zhang, X. Adsorption of MS2 on Oxide Nanoparticles Affects Chlorine Disinfection and Solar Inactivation. *Water Res.* **2015**, *69*, 59−67.
(35) Zhang, W.; Chen, Y. Experimental Determination of Conduction and Valence Bands of Semiconductor Nanoparticles using Kelvin Probe Force Microscopy. *J. Nanopart. Res.* **2012**, *14*, 1334.
(36) Xia, F.; Zhu, Y.; Feng, L.; Jiang, L. Smart Responsive Surfaces Switching Reversibly Between Super-Hydrophobicity and Super-Hydrophilicity. *Soft Matter* **2009**, *5*, 275−281.
(37) Yang, J.; Zhang, Z.; Men, X.; Xu, X.; Zhu, X. Reversible Superhydrophobicity to Superhydrophilicity Switching of a Carbon Nanotube Film via Alternation of UV Irradiation and Dark Storage. *Langmuir* **2010**, *26*, 10198−10202.
(38) Huang, Y.; Chen, X.; Zhang, M. Q. Reversible Surface Wettability Conversion of Graphene Films: Optically Controlled Mechanism. *J. Mater. Sci.* **2014**, *49*, 3025−3033.

DOI: 10.1021/acsami.5b03472
ACS Appl. Mater. Interfaces 2015, 7, 11677−11682